Hindawi
Journal of Nanomaterials
Volume 2023, Article ID 6279023, 10 pages
https://doi.org/10.1155/2023/6279023

Research Article

Insight into Perovskite Solar Cell Formation for Various Organohalides Perovskite Precursors in the Presence of Water at the Molecular Level

Sultan Zhantuarov,[1] Ainagul Kemelbekova,[1] Aigul Shongalova,[1] Kazybek Aimaganbetov,[1] Zhassulan Sailau,[2] Anuar Aldongarov,[3] Abay Serikkanov,[1] Nikolay Chuchvaga,[1] and Nurlan Almas[4]

[1]*Institute of Physics and Technology, Satbayev University, Almaty 050032, Kazakhstan*
[2]*Department of Chemistry and Chemical Technology, Al-Farabi Kazakh National University, Almaty 050000, Kazakhstan*
[3]*Department of Technical Physics, L. N. Gumilyov Eurasian National University, Astana 010000, Kazakhstan*
[4]*International Science Complex Astana, Institute for Hydrogen Energy, Astana 010000, Kazakhstan*

Correspondence should be addressed to Nurlan Almas; nurlanalmasov@gmail.com

Received 24 March 2023; Revised 22 May 2023; Accepted 7 June 2023; Published 19 June 2023

Academic Editor: Sivasankar Koppala

Copyright © 2023 Sultan Zhantuarov et al. This is an open access article distributed under the Creative Commons Attribution License, which permits unrestricted use, distribution, and reproduction in any medium, provided the original work is properly cited.

Recently, hybrid (organic–inorganic) metal halide perovskites have gained significant attention due to their excellent performance in optoelectronics and photovoltaics (PV). Single-junction PV cells made from these materials have achieved record efficiencies of over 25%, with the potential for further improvement in the future. The crystal structure of organohalide perovskite semiconductors plays a crucial role in the success of perovskites. In this study, we used classical all-atom molecular dynamics simulations to investigate the dynamics of ionic precursors as they form organic halide perovskite units in the presence of water as a solvent. During the analysis of radial distribution functions, interaction energies, hydrogen bonding, and diffusion coefficients, it was confirmed that organic precursors aggregate in the absence of water and disperse in the presence of water. The interaction energies also showed that the organic precursors of the perovskite have weaker interactions with Pb than the other components of the perovskite. The hydrogen bonding analysis revealed that the number of hydrogen bonds between the organic precursors and Cl decreases in the presence of water, but hydrogen bonds form between the organic precursors/water and Cl/water. Additionally, the diffusion coefficients of the organic precursors were found to be in the following increasing order: 2,2-(ethylenedioxy) bis ethylammonium ($EDBE^{2+}$) < guanidium (GA^{+}) < phenethylammonium (PEA^{+}) < iso-butylammonium ($Iso\text{-}BA^{+}$).

1. Introduction

Organic–inorganic metal halide perovskites have gained significant interest due to their high efficiency, high absorption coefficient, high defect tolerance, low cost, and ease of preparation in optoelectronics and photovoltaics devices [1–6]. The most common hybrid perovskites are methylammonium lead triiodide ($CH_3NH_3PbI_3$ or $MAPbI_3$) and formamidinium lead triiodide ($CH_5N_2PbI_3$ or $FAPbI_3$). Single junction perovskite solar cells (PSCs) have achieved record efficiencies of over 25.2% [7], and tandem silicon/PSCs have reached 29.8% [8]. One of the major advantages of perovskite films is their ability to be prepared using low-energy intensity techniques, such as spin coating, tape casting, and antisolvent dropping [9–11]. Although organic–inorganic metal halide perovskites have many positive qualities, they have not yet been widely commercialized due to their toxic components and unstable nature. These toxic materials can cause environmental pollution when disposed of, and the perovskites' efficiency can also decrease over time due to the decomposition of their hydrophilic organic components when exposed to the environment. Currently, researchers are working on finding ways to replace these toxic materials while maintaining the effectiveness of the devices.

The photoactivity of $CH_3NH_3PbI_3$ and $CH_5N_2PbI_3$ decreases quickly in humid conditions due to the decomposition of

their methylammonium and methylamine cations, respectively [12]. This makes the photochemical stability of organic–inorganic metal halide hybrid perovskite solar cells (PSCs) relatively poor compared to traditional organic and inorganic semiconductors [13]. There have been various methods developed to improve stability, including interface engineering, additive engineering, passivating defects, stabilizing heterostructures, and encapsulating cells [14–20]. Among the various strategies using long-chain hydrophobic organic cations, such as butylammonium, ethylammonium, dodecylammonium, 2-(2-pyridyl) ethylamine, hydrazinium, trimethylammonium, and phenylethyl ammonium, have shown promise [20–25]. Low-dimensional structures (2D) formed by long-chain hydrophobic organic cations make them more stable.

Perovskite solar cells that are based solely on low-dimensional structures have low efficiency due to their wide bandgap and low absorption. An early study on 2D devices using $(PEA)_2(MA)_2[Pb_3I_{10}]$ demonstrated an efficiency of only 4.73% [25]. However, using a combination of 2D and 3D structures, or conventional hybrid perovskites, can improve the efficiency of 2D/3D mixed devices. At present, dual-optimized 2D@3D/2D devices have shown the highest efficiency of 23.2% when 2-(2-pyridyl)ethylamine (2-PyEA) molecules with 2D structure and N atoms with a lone electron pair are introduced into perovskite [21]. However, these devices are slightly less efficient compared to conventional 3D devices.

According to the data from previous research, the crystal structure needs to be modified in order to improve the movement of charge carriers in 2D/3D devices. The incorporation of a 2D structure into 3D solar cells is a relatively recent development, and further research is needed to identify structures that can withstand the effects of oxygen, moisture, light, and temperature. To achieve this, it will be necessary to study the photophysical processes and electronic properties in greater detail and develop appropriate strategies. Herein, molecular dynamics (MD) simulations are useful for studying the formation of crystals in various materials, as they can model systems with thousands of atoms and account for concentration and solvent effects. These simulations typically use Lennard–Jones (LJ) potentials to describe the interactions between atoms. Currently, MD modeling and simulation techniques have not been applied to study the formation of PSCs made from various organohalides.

In this work, classical all-atom MD simulations were performed to study the intermolecular interactions within the ionic precursors and to explore the organic halide perovskite formation in the presence of solvent molecules. In particular, we have selected various organic precursors, that is, iso-butylammonium, phenethylammonium, 2,2-(ethylenedioxy) bis ethylammonium, and guanidium to understand the organic halide perovskite formation process in the presence of aqueous media. The choice of the organic halides depends on the available experimental and simulation parameters, as we explained below. In the following sections, the classical all-atom MD simulation methodologies, radial distribution functions, interaction energies, hydrogen bonds, and diffusion coefficients were described in detail.

Table 1: Simulation details for the various organohalides perovskite precursors in the water.

	Designed systems	Pb	Cl	Organohalides	Water
1	Reference	20	40	–	–
2	Iso-BA^+	20	60	20	–
3		20	60	20	500
4	PEA^+	20	60	20	–
5		20	60	20	500
6	$EDBE^{2+}$	20	80	20	–
7		20	80	20	500
8	GA^+	20	60	20	–
9		20	60	20	500

2. Methodology

In order to study the formation of PSC, different MD simulations were designed systematically. The actual PSC is highly complex. At the same time, the main purpose of this work is to study the formation mechanism of PSCs in the presence of various organohalides. In this regard, several organohalides, including iso-butylammonium (iso-BA^+), phenethylammonium (PEA^+), 2,2-(ethylenedioxy) bis ethylammonium ($EDBE^{2+}$), and guanidium (GA^+), were selected for the analysis. The choice of iso-BA^+ (iso-butylammonium), PEA^+ (phenethylammonium), $EDBE^{2+}$ (2,2-(ethylenedioxy) bis ethylammonium), and GA^+ (guanidium) in the MD simulations instead of the simplest option of MA^+ (methylammonium) can be explained due to (i) chemical diversity: the impact of their chemical structures and properties on the perovskite formation process, (ii) tunability of properties: different organic cations can offer tunability in terms of their molecular size, shape, and polarizability, (iii) experimental relevance: Iso-BA^+, PEA^+, $EDBE^{2+}$, and GA^+ are organic cations that have been experimentally investigated or proposed for use in PSCs, (iv) comparative analysis: the inclusion of multiple organic cations allows for a comparative analysis of their performance and behavior within the perovskite structure. Consequently, there were nine designed systems, which are listed in Table 1.

A mixture of organic halides and lead halides was taken as a representative model of perovskite (Figure 1). After that, the optimized coordinates for the iso-butylammonium (iso-BA^+), phenethylammonium (PEA^+), 2,2-(ethylenedioxy) bis ethylammonium ($EDBE^{2+}$), and guanidium (GA^+) were obtained from the ATB database. The LJ parameters and other optimized force field parameters for the standard CHARMM force field were generated using SwissParam. The optimized force field parameters and charges for the lead and chloride ions were taken from the standard CHARMM force field database. The SPC model was used as an example and included explicitly added water molecules.

To begin, a $5 \times 5 \times 5\ nm^3$ was used for an initial simulation with a maximum force of 500 kJ/mol/nm on any atom, all at a temperature of 298 K and pressure of 1 bar. The energy was then minimized. Following this, the temperature and pressure were held constant at 298 K and 1 bar, respectively,

9182, 2023, 1, Downloaded from https://onlinelibrary.wiley.com/doi/10.1155/2023/6279023 by INASP/HINARI - KAZAKHSTAN, Wiley Online Library on [01/04/2026]. See the Terms and Conditions (https://onlinelibrary.wiley.com/terms-and-conditions) on Wiley Online Library for rules of use; OA articles are governed by the applicable Creative Commons License

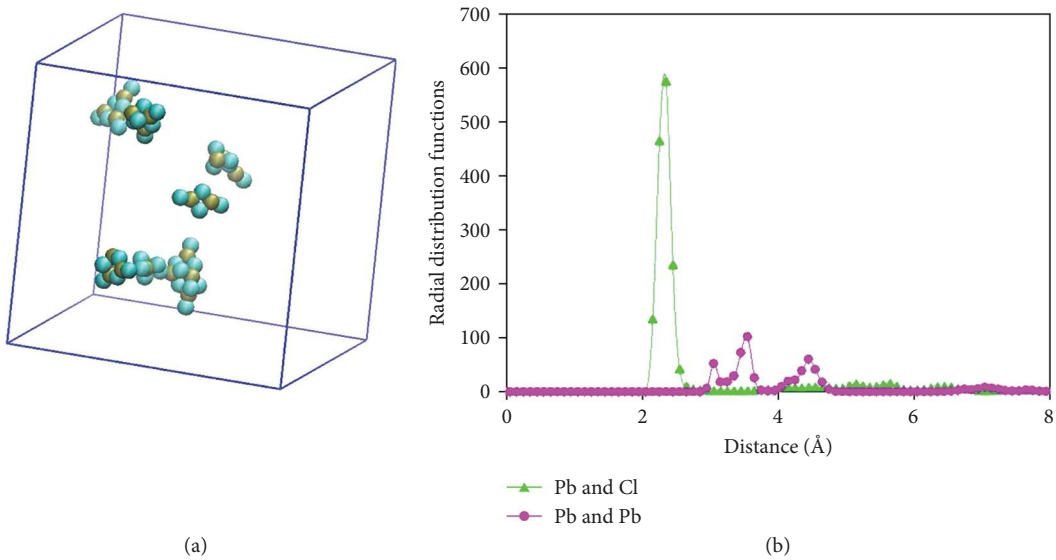

Figure 1: Representative snapshots and radial distribution functions of lead(II) chloride ((a) and (b)).

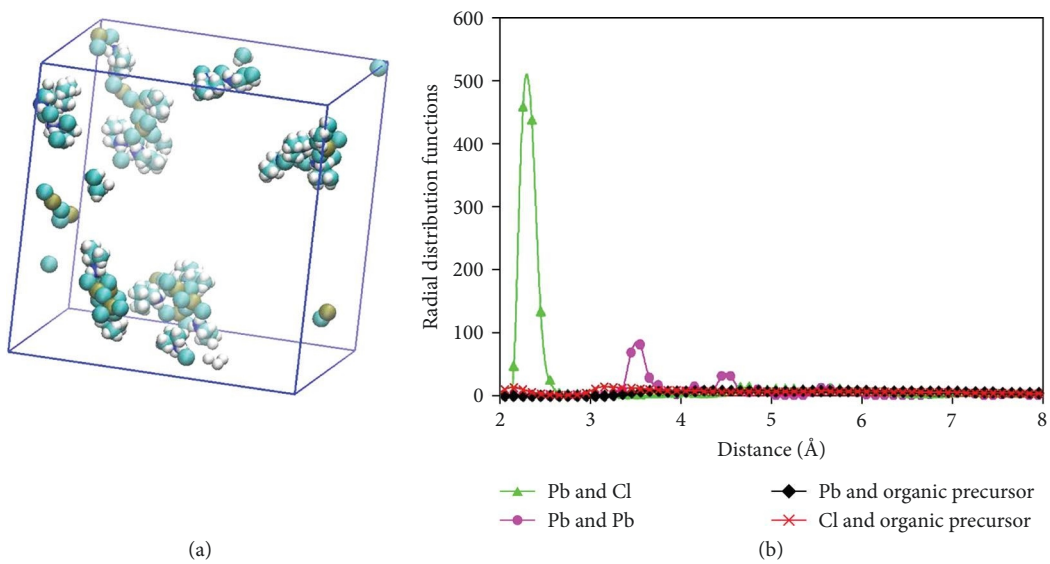

Figure 2: Representative snapshots and radial distribution functions of lead(II) chloride + iso-BA^+ ((a) and (b)).

for 0.1 ns during canonical ensemble equilibration, where constant amount of substance (N), volume (V), and temperature (T) are conserved. Finally, MD simulations were run for a duration of 10 ns at a temperature of 298 K and pressure of 1 bar.

The linear constraint solver algorithm was used to constrain all bonds during the simulation. The particle mesh Ewald summation method, using a fourth-order and 0.16 nm grid spacing, was used to calculate long-range interactions. The V-rescale method was utilized to maintain the temperature, and Berendsen pressure coupling was employed to maintain the pressure of the system. Additionally, periodic boundary conditions were applied [26, 27].

In general, there were nine designed systems of PSCs in the presence of various organohalides. In this regard, several organohalides, including iso-BA^+, PEA^+, $EDBE^{2+}$, and GA^+, are illustrated in Table 1. The analyses of classical all-atom MD simulations were performed by obtaining radial distribution functions, interaction energies, and the number of hydrogen bonds. The classical all-atom MD simulations are performed by the Gromacs software [28] and visualized by the visual molecular dynamics package [29].

3. Results and Discussion

3.1. Molecular Structural Properties. The equilibrated classical all-atom MD simulations for lead(II) chloride with precursors in the presence and absence of water are illustrated in Figures 1–9. Initially, it was found that the organic precursors are aggregated in the absence of water. Furthermore, it was observed that when water was absent, the clustering of

9182, 2023, 1, Downloaded from https://onlinelibrary.wiley.com/doi/10.1155/2023/6279023 by INASP/HINARI - KAZAKHSTAN, Wiley Online Library on [01/04/2026]. See the Terms and Conditions (https://onlinelibrary.wiley.com/terms-and-conditions) on Wiley Online Library for rules of use; OA articles are governed by the applicable Creative Commons License

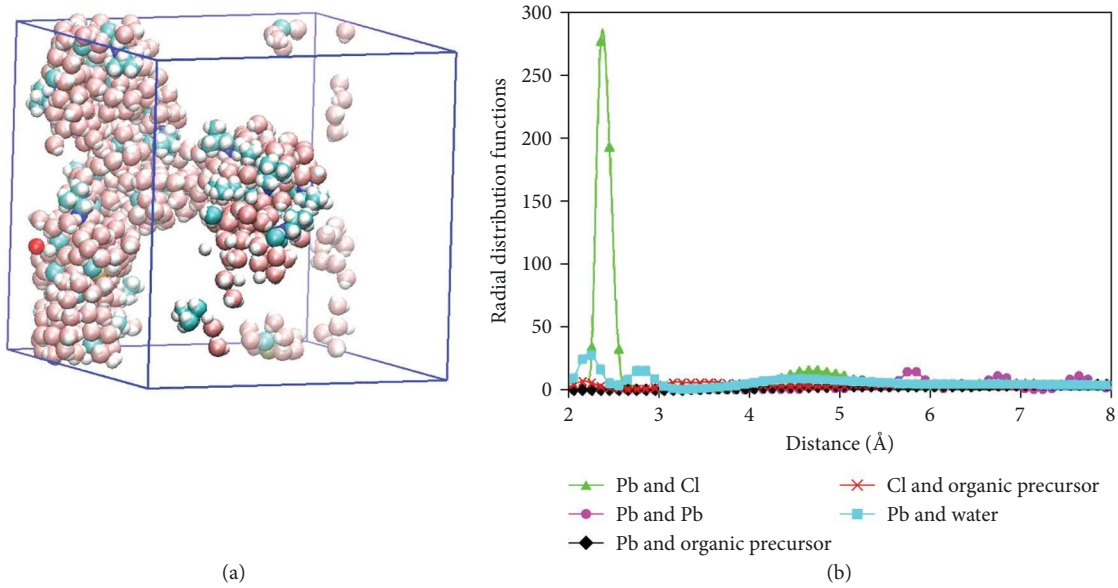

Figure 3: Representative snapshots and radial distribution functions of lead(II) chloride + iso-BA$^+$ + water ((a) and (b)).

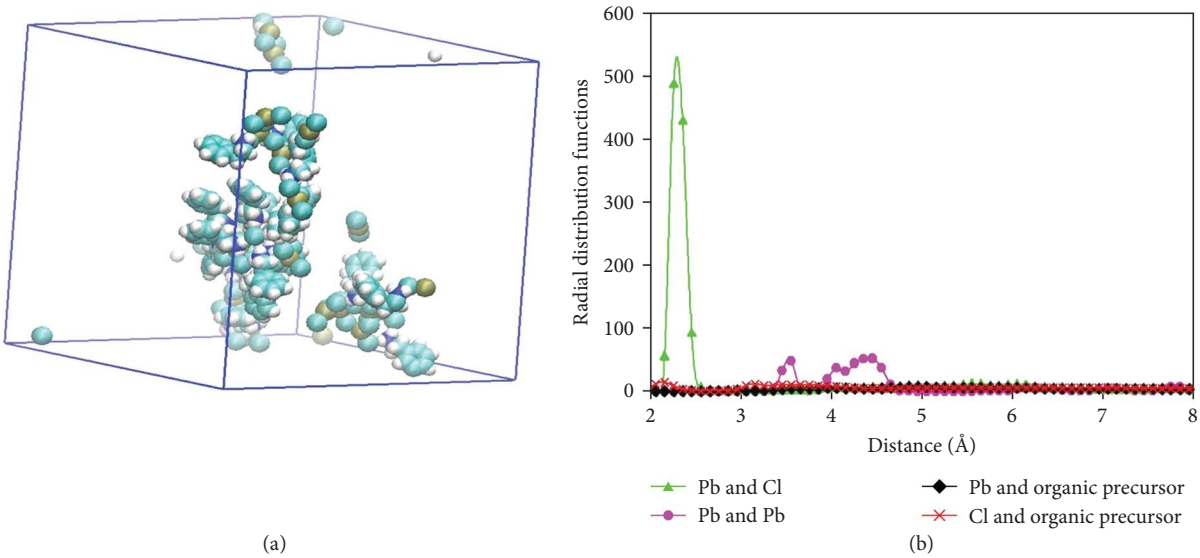

Figure 4: Representative snapshots and radial distribution functions of lead(II) chloride + PEA$^+$ ((a) and (b)).

organic precursors persisted over time, but the aggregates were broken up in the presence of water. In fact, the organic precursor ions were found to be highly solvated and dispersed when water was present. This can be attributed to the polar nature of water molecules and the ionic behavior of the organic precursors, as shown in Figures 1–9.

In Figures 1–9, the radial distribution functions between Pb, Cl, organic precursor, and water are reported. It can be highlighted that there is practically no correlation between lead and organic precursors. On the contrary, for Cl and organic precursor, a smaller peak is detected. Accordingly, the coordination is more pronounced for Pb and Cl interaction. In the absence and presence of water, the first coordination peak reaches a value of around 100. In addition, the Pb and Pb, and Pb with water had a moderate peak distance at different precursors.

Moreover, from the weak interactions between Pb and organic precursors, it can be observed that the organic precursors of the perovskite are less interacted than the rest of the components of the perovskite. Pb and Cl ions tend to "freeze" in a relatively robust $PbCl_x$–$PbCl_x$ framework and, the microscopic structure of the methylammonium cations remains more liquid-like, as can be seen in Figures 1–9. The predictions of the classical all-atom MD simulations in water medium are consistent with experimental findings.

After the analysis of radial distribution functions, classical all-atom MD simulations were performed to study the intermolecular interactions within lead chloride-containing perovskite

9182, 2023, 1, Downloaded from https://onlinelibrary.wiley.com/doi/10.1155/2023/6279023 by INASP/HINARI - KAZAKHSTAN, Wiley Online Library on [01/04/2026]. See the Terms and Conditions (https://onlinelibrary.wiley.com/terms-and-conditions) on Wiley Online Library for rules of use; OA articles are governed by the applicable Creative Commons License

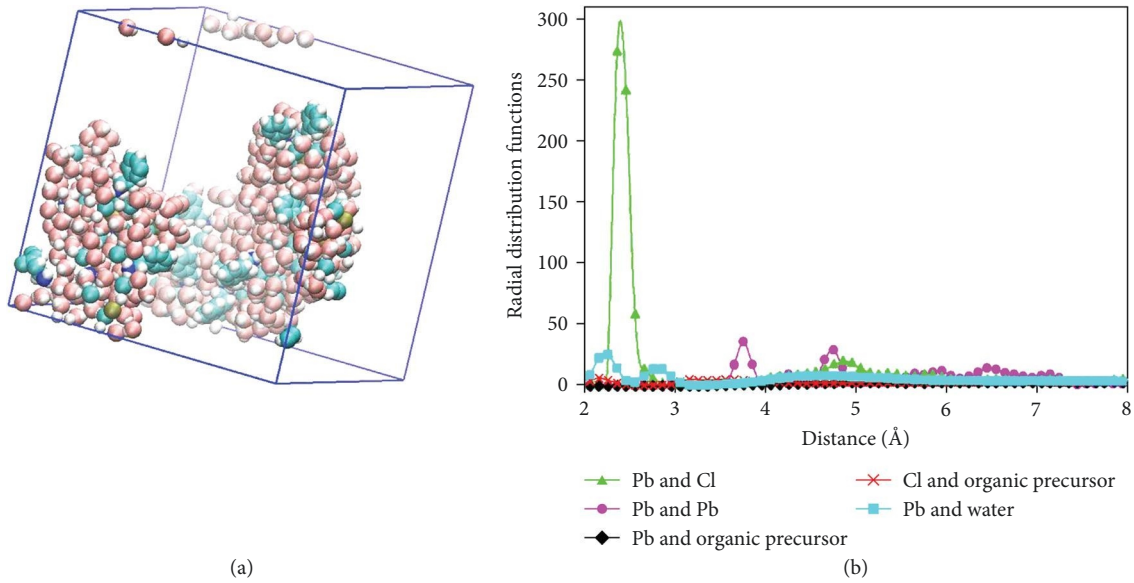

Figure 5: Representative snapshots and radial distribution functions of lead(II) chloride + PEA^+ + water ((a) and (b)).

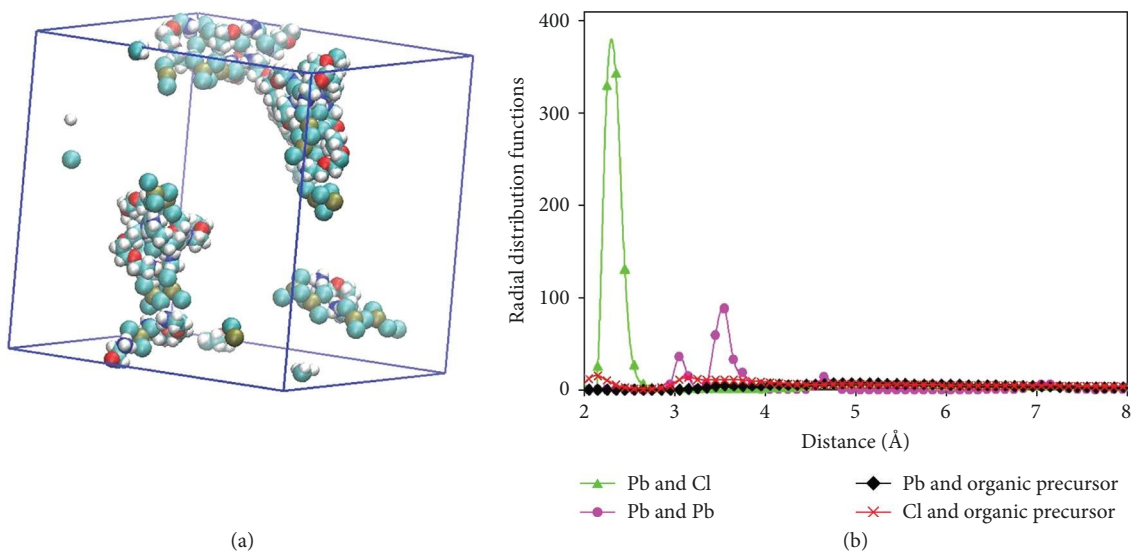

Figure 6: Representative snapshots and radial distribution functions of lead(II) chloride + $EDBE^{2+}$ ((a) and (b)).

in the presence of different organic precursors. We continue the analysis by examining the interaction energies between the components. In particular, the interactions of Pb(II) ion with organic precursor compounds, including iso-BA^+, PEA^+, $EDBE^{2+}$, and GA^+ in the absence and presence of water, were evaluated. The interaction energies were computed as the sum of short-range LJ and columbic interactions between the molecules. The energies reported are the average values over the last 2 ns of the production run. The standard deviation for all obtained data was less than 1%. Table 2 reports energies between different components for all nine systems.

Comparison between the interaction energies in the presence and absence of organic precursor and water showed that organic precursor and water directly affect the intermolecular interaction energies of Pb and Cl case. For instance, by comparing systems 1 and 2, we found that the intermolecular interaction between Pb and Cl decreased from −160.45 to −219.68 kJ/mol. Moreover, interaction energies between Pb and Cl increased in the presence of water in comparison with the absence of water.

Next, the hydrogen bond is present in many chemical systems, and consequently, it is the highly important for describing the intermolecular interactions of molecules. Therefore, the formation of perovskite is, in general, explained in terms of hydrogen bonds, as can be seen in Table 3. Hence, in order to compute the number of hydrogen bonds, geometric criteria were employed herein, the distance between the donor and acceptor should be less than 0.35 nm, and the angle should be within 300.

The results, as shown in Table 3, revealed that the number of hydrogen bonds between organic precursors and Cl was decreased in the presence of water, as can be seen in

9182, 2023, 1, Downloaded from https://onlinelibrary.wiley.com/doi/10.1155/2023/6279023 by INASP/HINARI - KAZAKHSTAN, Wiley Online Library on [01/04/2026]. See the Terms and Conditions (https://onlinelibrary.wiley.com/terms-and-conditions) on Wiley Online Library for rules of use; OA articles are governed by the applicable Creative Commons License

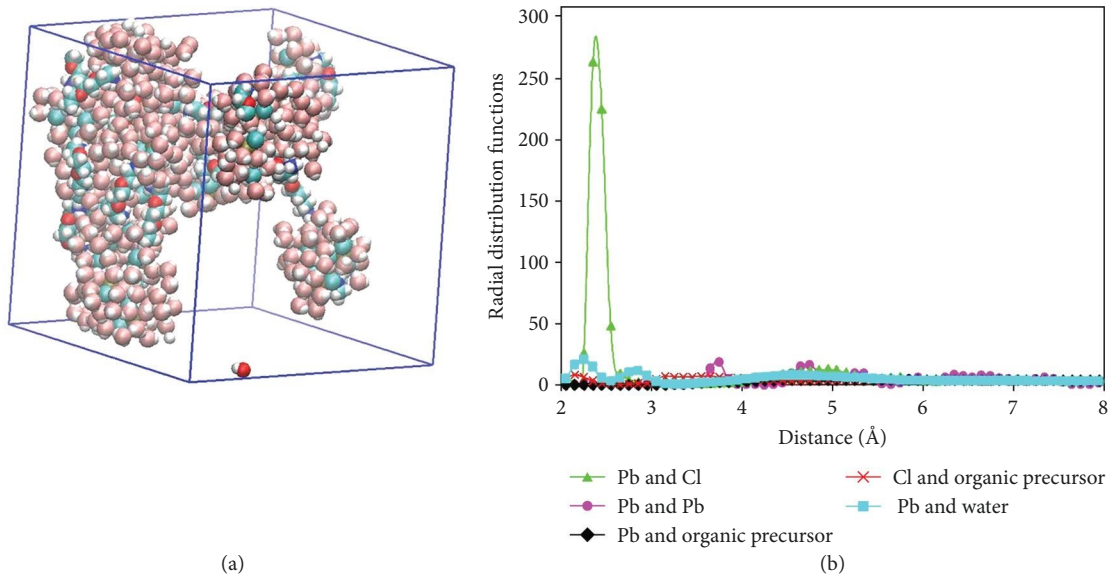

Figure 7: Representative snapshots and radial distribution functions of lead(II) chloride + $EDBE^{2+}$ + water ((a) and (b)).

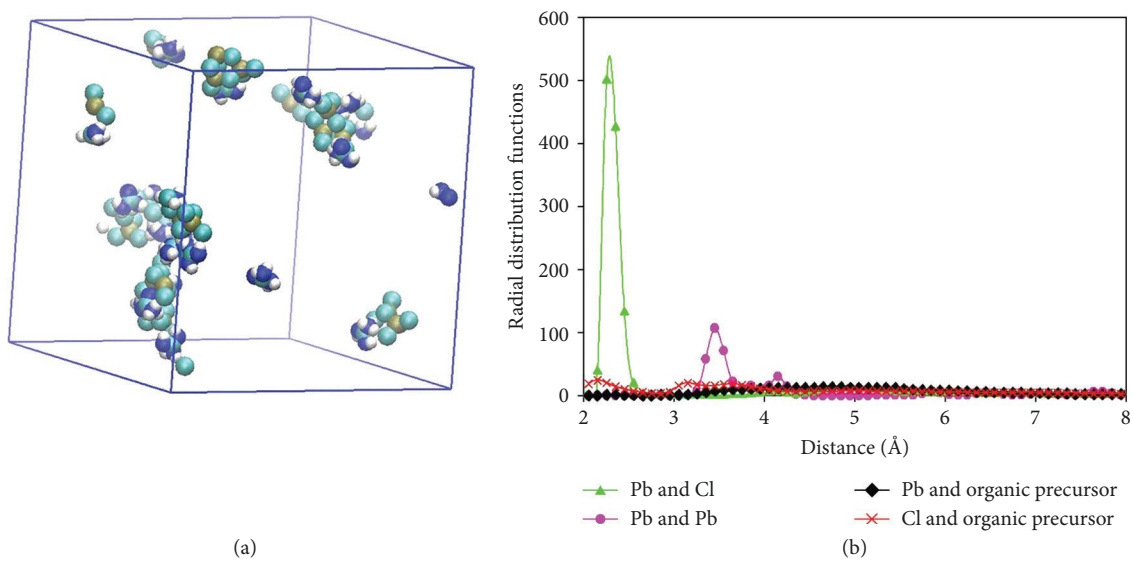

Figure 8: Representative snapshots and radial distribution functions of lead(II) chloride + GA^+ ((a) and (b)).

systems 2–9. Moreover, we can note a formation of hydrogen bondings between organic precursors/water and Cl/water in systems in systems 3, 5, 7, and 9. At the same time, strong hydrogen bonding was observed between organic precursor/Cl ion. In addition, the electrostatic interactions are dominated inside charged particles of lead halide PSC and could have lower hydrogen bonds [30–32]. At the same time, the crystal dimensions could be manipulated with the collective effects of hydrogen bonding in various lead halide perovskite [33, 34]. In this regard, better hydrogen-bonded lead halide perovskite crystals could yield a better stability toward lights and moisture.

3.2. Dynamic Properties. The diffusion coefficients were computed using Einstein–Smoluchowski equation. Diffusion coefficients of the Pb, Cl, organic precursors, and water for all nine simulation systems are illustrated in Table 4. As can be seen from Table 4, the diffusion coefficients of Pb and Cl were decreasing dramatically from systems 1 to 7.

At the same time, the diffusion coefficients of organic precursors were in the following increasing order: $EDBE^{2+} < GA^+ < PEA^+ < Iso\text{-}BA^+$. While the diffusivity of water was in the following increasing order: $PEA^+ < EDBE^{2+} < Iso\text{-}BA^+ < GA^+$. Herein, it can be noted that the lead halide perovskites are a better conductor of ions [35]. In addition, the intrinsic defects can migrate in lead halide perovskite lattice. Moreover, iodine anion migration also was noted via vacancies and organic cation displacement in lead halide perovskite lattice according to the previously studied density functional theory calculations [36–38].

9182, 2023, 1, Downloaded from https://onlinelibrary.wiley.com/doi/10.1155/2023/6279023 by INASP/HINARI - KAZAKHSTAN, Wiley Online Library on [01/04/2026]. See the Terms and Conditions (https://onlinelibrary.wiley.com/terms-and-conditions) on Wiley Online Library for rules of use; OA articles are governed by the applicable Creative Commons License

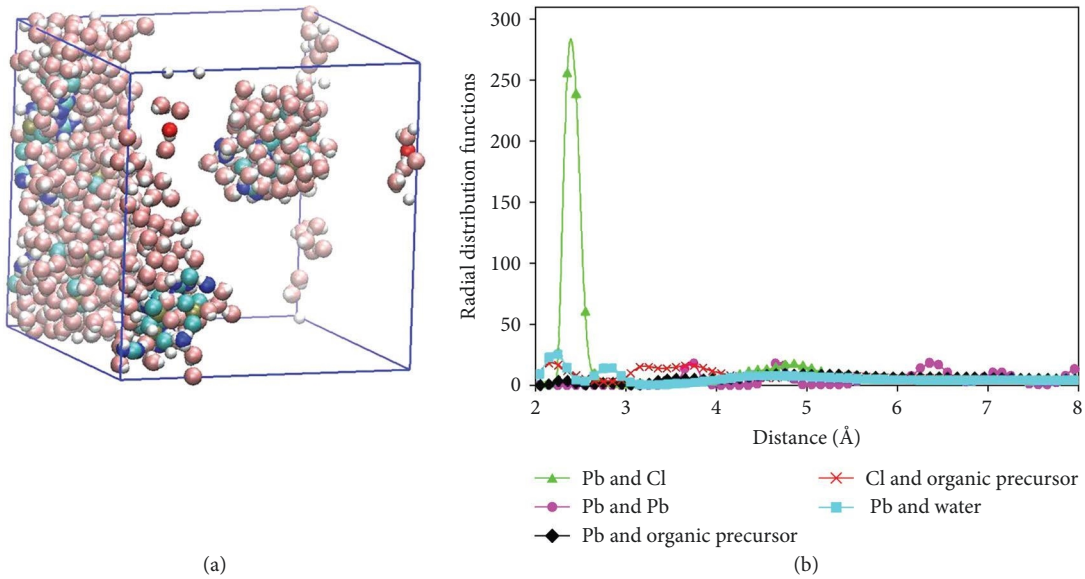

Figure 9: Representative snapshots and radial distribution functions of lead(II) chloride + GA + water ((a) and (b)).

Table 2: Interaction energies for the various organohalides perovskite precursors in the water.

	System name	Pb and Cl	Pb and organic precursor	Pb and water	Organic precursor and Cl	Organic precursor and water	Cl and water
1	Reference	−160.45	–	–	–	–	–
2	Iso-BA$^+$	−219.68	15.09	–	−58.18	–	–
3		−404.64	2.19	−1,951.36	−63.40	−254.04	−734.61
4	PEA$^+$	−111.57	7.16	–	−63.77	–	–
5		−507.32	2.15	−1,799.12	−69.14	−267.21	−629.03
6	EDBE^{2+}	−303.1	17.53	–	−114.41	–	–
7		−616.04	7.28	−1,520.38	−158.52	−423.67	−840.53
8	GA$^+$	−219.27	−12.55	–	−51.03	–	–
9		−485.36	−44.60	−1,800.82	−97.94	−483.51	−554.94

Unit: kJ/mol.

Table 3: Number of hydrogen bondings for the interactions of various organohalide perovskite precursors in the water.

	System name	Organic precursor and Cl	Organic precursor and water	Cl and water
1	Reference	–	–	–
2	Iso-BA$^+$	26	–	–
3		17	52	356
4	PEA$^+$	40	–	–
5		18	59	310
6	EDBE^{2+}	77	–	–
7		43	88	393
8	GA$^+$	36	–	–
9		30	87	293

Table 4: Diffusion coefficients for the various organohalides perovskite precursors in the water.

	System name	Pb	Cl	Organic precursor	Water
1	Reference	0.0221	0.0223	–	–
2	Iso-BA$^+$	0.0003	0.0002	0.0016	–
3		0.00001	0.0047	0.0758	0.9906
4	PEA$^+$	0.0001	0.00012	0.0012	–
5		0.0002	0.0107	0.0551	0.3740
6	EDBE^{2+}	0.0001	0.0001	0.0002	–
7		0.00001	0.0040	0.0114	0.6991
8	GA$^+$	0.00001	0.0002	0.0022	–
9		0.00001	0.0032	0.0129	1.0165

Unit: $\times 10^{-5}$ cm^2/s.

Desirable characteristics of organohalide perovskite materials encompass luminescence and optical behavior, electrical conductivity, ease of processing, and flexibility, as well as stability [39]. By studying the diffusion coefficients of the organic precursor species of lead halide perovskite, researchers can assess the likelihood of diffusion-driven processes that may lead to degradation or instability. Lower diffusion coefficients found in MD simulations could suggest that the material system has enhanced stability. Herein, Iso-BA$^+$ and PEA$^+$ yielded a higher mobility in comparison with EDBE^{2+} and GA$^+$, which

9182, 2023, 1, Downloaded from https://onlinelibrary.wiley.com/doi/10.1155/2023/6279023 by INASP/HINARI - KAZAKHSTAN, Wiley Online Library on [01/04/2026]. See the Terms and Conditions (https://onlinelibrary.wiley.com/terms-and-conditions) on Wiley Online Library for rules of use; OA articles are governed by the applicable Creative Commons License

could mean their lower stability in the presence of water solvent. However, it is important to note that diffusion coefficients alone may not provide a complete picture of stability. Other factors, such as the thermodynamic properties, intermolecular interactions, and kinetic barriers, also play crucial roles in determining the overall stability of PSCs [40–42]. Therefore, a comprehensive understanding of the organic PSC behavior is also planned to study in the future by applying experimental techniques and more advanced modeling and simulation techniques via understanding relative energy levels and absorption data.

4. Conclusion

In summary, classical all-atom MD simulations were used to study the dynamics of ionic precursors as they form organic halide perovskite units in the presence of solvent molecules. The radial distribution functions between Pb and organic halide showed that the organic precursors of the perovskite have weaker chemical interactions with Pb than the other components of the perovskite. Pb and Cl ions tend to "freeze" in a relatively stable $PbCl_x$–$PbCl_x$ framework. Analysis of interaction energies indicated that the interaction energies between Pb and Cl are stronger in the presence of water than in its absence.

MD analysis revealed that the interaction between the organic precursor and organic halides is due to hydrogen bonding. Halide perovskites are good ion conductors, and the mobility of the organic precursors was found to be in the following increasing order: $EDBE^{2+} < GA^{+} < PEA^{+} < Iso\text{-}BA^{+}$. Herein, $Iso\text{-}BA^{+}$ and PEA^{+} yielded an improved diffusion in comparison with $EDBE^{2+}$ and GA^{+}, which can mean their lower stability in the presence of water solvent. However, it is important to note that diffusion coefficients alone may not provide a complete picture of stability. This research can help to understand the formation mechanisms of organic halide PSCs at the molecular level and may aid in the molecular design of PSCs with improved stability performance. Future research endeavors will focus on gaining a thorough comprehension of the behavior of organic PSCs. This will involve employing experimental methods as well as employing advanced modeling and simulation techniques to better understand the correlation between energy levels and absorption data.

Abbreviations

PV: Photovoltaics
Pb: Lead
Cl: Chloride ion
$EDBE^{2+}$: 2,2-(Ethylenedioxy) bis ethylammonium
GA^{+}: Guanidium
PEA^{+}: Phenethylammonium
$Iso\text{-}BA^{+}$: Iso-butylammonium
PSC: Perovskites solar cells
MD: Molecular dynamics.

Data Availability

The datasets generated during and/or analyzed during the current study are available from the corresponding author upon reasonable request.

Additional Points

Highlights. (i) The dynamics of ionic precursors toward organic halide perovskite unit formation in the presence of solvent molecules were studied via classical all-atom molecular dynamics simulations. (ii) From the weak interactions between Pb and organic precursors, it can be observed that the organic precursors of the perovskite are less interacted than the rest of the components of the perovskite according to the interaction energies as well. (iii) At the same time, the diffusion coefficients of organic precursors were in the following increasing order: $EDBE^{2+} < GA^{+} < PEA^{+} < Iso\text{-}BA^{+}$.

Disclosure

MD simulations were performed using the Gromacs program package.

Conflicts of Interest

The authors declare that they have no conflicts of interest.

Authors' Contributions

Sultan Zhantuarov: writing—review and editing; Ainagul Kemelbekova: conceptualization, methodology, formal analysis, writing—original draft; Aigul Shongalova: formal analysis, writing—review and editing; Kazybek Aimaganbetov: methodology, writing—review and editing; Zhassulan Sailau: methodology, writing—review and editing; Anuar Aldongarov: formal analysis, writing—review and editing; Abay Serikkanov: conceptualization, writing—review and editing; Nikolay Chuchvaga: conceptualization, funding acquisition, writing—review and editing; Nurlan Almassov: conceptualization, writing—review and editing.

Acknowledgments

This research was funded by the Committee of Science of the Ministry of Education and Science of the Republic of Kazakhstan via grant #AP09260940. Anuar Aldongarov acknowledges the support from the Ministry of Education and Science of the Republic of Kazakhstan via grant #AP08052504. Nurlan Almas gratefully acknowledges the support from the Ministry of Education and Science of the Republic of Kazakhstan via grant #AP14871389. Also, the authors acknowledge the support of the Department of Physics and Technology and Laboratory of Physical and Quantum Chemistry of L. N. Gumilyov Eurasian National University for providing us with computational resources.

9182, 2023, 1, Downloaded from https://onlinelibrary.wiley.com/doi/10.1155/2023/6279023 by INASP/HINARI - KAZAKHSTAN, Wiley Online Library on [01/04/2026]. See the Terms and Conditions (https://onlinelibrary.wiley.com/terms-and-conditions) on Wiley Online Library for rules of use; OA articles are governed by the applicable Creative Commons License

References

[1] J. Y. Kim, J.-W. Lee, H. S. Jung, H. Shin, and N.-G. Park, "High-efficiency perovskite solar cells," *Chemical Reviews*, vol. 120, no. 15, pp. 7867–7918, 2020.

[2] M. A. Ghebouli, B. Ghebouli, L. Krache et al., "Prediction study of the structural, elastic, electronic, dynamic, optical and thermodynamic properties of cubic perovskite $BiGaO_3$," *Bulletin of Materials Science*, vol. 45, Article ID 124, 2022.

[3] M. A. Mahmud, T. Duong, J. Peng et al., "Origin of efficiency and stability enhancement in high-performing mixed dimensional 2D–3D perovskite solar cells: a review," *Advanced Functional Materials*, vol. 32, no. 3, Article ID 2009164, 2022.

[4] A. Kojima, K. Teshima, Y. Shirai, and T. Miyasaka, "Organometal halide perovskites as visible-light sensitizers for photovoltaic cells," *Journal of the American Chemical Society*, vol. 131, no. 17, pp. 6050-6051, 2009.

[5] M. Faizan, G. Murtaza, S. H. Khan et al., "First-principles study of the double perovskites Sr_2XOsO_6 (X = Li, Na, Ca) for spintronics applications," *Bulletin of Materials Science*, vol. 39, pp. 1419–1425, 2016.

[6] L. Kong, X. Zhang, Y. Li et al., "Smoothing the energy transfer pathway in quasi-2D perovskite films using methanesulfonate leads to highly efficient light-emitting devices," *Nature Communications*, vol. 12, Article ID 1246, 2021.

[7] J. Jeong, M. Kim, J. Seo et al., "Pseudo-halide anion engineering for α-$FAPbI_3$ perovskite solar cells," *Nature*, vol. 592, pp. 381–385, 2021.

[8] P. Tockhorn, J. Sutter, A. Cruz et al., "Nano-optical designs for high-efficiency monolithic perovskite–silicon tandem solar cells," *Nature Nanotechnology*, vol. 17, pp. 1214–1221, 2022.

[9] X. Liu, X. Tan, Z. Liu et al., "Boosting the efficiency of carbon-based planar $CsPbBr_3$ perovskite solar cells by a modified multistep spin-coating technique and interface engineering," *Nano Energy*, vol. 56, pp. 184–195, 2019.

[10] D. Bryant, P. Greenwood, J. Troughton et al., "A transparent conductive adhesive laminate electrode for high-efficiency organic–inorganic lead halide perovskite solar cells," *Advanced Materials*, vol. 26, no. 44, pp. 7499–7504, 2014.

[11] K.-M. Lee, C.-J. Lin, B.-Y. Liou et al., "Selection of anti-solvent and optimization of dropping volume for the preparation of large area sub-module perovskite solar cells," *Solar Energy Materials and Solar Cells*, vol. 172, pp. 368–375, 2017.

[12] J. Yang, B. D. Siempelkamp, D. Liu, and T. L. Kelly, "Investigation of $CH_3NH_3PbI_3$ degradation rates and mechanisms in controlled humidity environments using *in situ* techniques," *ACS Nano*, vol. 9, no. 2, pp. 1955–1963, 2015.

[13] A. Binek, F. C. Hanusch, P. Docampo, and T. Bein, "Stabilization of the trigonal high-temperature phase of formamidinium lead iodide," *The Journal of Physical Chemistry Letters*, vol. 6, no. 7, pp. 1249–1253, 2015.

[14] Z. Yang, J. Dou, S. Kou et al., "Multifunctional phosphorus-containing Lewis acid and base passivation enabling efficient and moisture-stable perovskite solar cells," *Advanced Functional Materials*, vol. 30, no. 15, Article ID 1910710, 2020.

[15] K. Wang, J. Liu, J. Yin et al., "Defect passivation in perovskite solar cells by cyano-based π-conjugated molecules for improved performance and stability," *Advanced Functional Materials*, vol. 30, no. 35, Article ID 2002861, 2020.

[16] Y. Sha, E. Bi, Y. Zhang et al., "A scalable integrated dopant-free heterostructure to stabilize perovskite solar cell modules," *Advanced Energy Materials*, vol. 11, no. 5, Article ID 2003301, 2021.

[17] J. Peng, D. Walter, Y. Ren et al., "Nanoscale localized contacts for high fill factors in polymer-passivated perovskite solar cells," *Science*, vol. 371, pp. 390–395, 2021.

[18] X. Zheng, Y. Hou, C. Bao et al., "Managing grains and interfaces via ligand anchoring enables 22.3%-efficiency inverted perovskite solar cells," *Nature Energy*, vol. 5, pp. 131–140, 2020.

[19] L. K. Ono, S. Liu, and Y. Qi, "Reducing detrimental defects for high-performance metal halide perovskite solar cells," *Angewandte Chemie International Edition*, vol. 59, no. 17, pp. 6676–6698, 2020.

[20] B. Hailegnaw, S. Kirmayer, E. Edri, G. Hodes, and D. Cahen, "Rain on methylammonium lead iodide based perovskites: possible environmental effects of perovskite solar cells," *Journal of Physical Chemistry Letters*, vol. 6, no. 9, pp. 1543–1547, 2015.

[21] C. Zuo, A. D. Scully, W. L. Tan et al., "Crystallisation control of drop-cast quasi-2D/3D perovskite layers for efficient solar cells," *Communications Materials*, vol. 1, Article ID 33, 2020.

[22] G. Liu, H. Zheng, X. Xu et al., "Introduction of hydrophobic ammonium salts with halogen functional groups for high-efficiency and stable 2D/3D perovskite solar cells," *Advanced Functional Materials*, vol. 29, no. 47, Article ID 1807565, 2019.

[23] M. N. Shaikh, Q. Zafar, and A. Papadakis, "A study of electromagnetic light propagation in a perovskite-based solar cell *via* a computational modelling approach," *Bulletin of Materials Science*, vol. 42, Article ID 169, 2019.

[24] S. C. Ezike, A. B. Alabi, A. N. Ossai, and A. O. Aina, "Effect of tertiary butylpyridine in stability of methylammonium lead iodide perovskite thin films," *Bulletin of Materials Science*, vol. 43, Article ID 40, 2020.

[25] D. K. Mahato, A. Dutta, and T. P. Sinha, "Dielectric relaxation in double perovskite oxide, Ho_2CdTiO_6," *Bulletin of Materials Science*, vol. 34, pp. 455–462, 2011.

[26] M. Karibayev and D. Shah, "Comprehensive computational analysis exploring the formation of caprolactam-based deep eutectic solvents and their applications in natural gas desulfurization," *Energy & Fuels*, vol. 34, no. 8, pp. 9894–9902, 2020.

[27] D. Shah, M. Karibayev, E. K. Adotey, and A. M. Torkmahalleh, "Impact of volatile organic compounds on chromium containing atmospheric particulate: insights from molecular dynamics simulations," *Scientific Reports*, vol. 10, Article ID 17387, 2022.

[28] D. Van Der Spoel, E. Lindahl, B. Hess, G. Groenhof, A. E. Mark, and H. J. C. Berendsen, "GROMACS: fast, flexible, and free," *Journal of Computational Chemistry*, vol. 26, no. 16, pp. 1701–1718, 2005.

[29] W. Humphrey, A. Dalke, and K. Schulten, "VMD: visual molecular dynamics," *Journal of Molecular Graphics*, vol. 14, no. 1, pp. 33–38, 1996.

[30] B. S. Semwal and N. S. Panwar, "Dielectric properties of perovskite crystals," *Bulletin of Materials Science*, vol. 15, pp. 237–250, 1992.

[31] Y. Okamoto and P. A. Madden, "Structural study of molten lanthanum halides by X-ray diffraction and computer simulation techniques," *Journal of Physics and Chemistry of Solids*, vol. 66, no. 2–4, pp. 448–451, 2005.

[32] K. L. Svane, A. C. Forse, C. P. Grey et al., "How strong is the hydrogen bond in hybrid perovskites?" *The Journal of Physical Chemistry Letters*, vol. 8, no. 24, pp. 6154–6159, 2017.

[33] B.-B. Cui, Y. Han, B. Huang et al., "Locally collective hydrogen bonding isolates lead octahedra for white emission improvement," *Nature Communications*, vol. 10, Article ID 5190, 2019.

9182, 2023, 1, Downloaded from https://onlinelibrary.wiley.com/doi/10.1155/2023/6279023 by INASP/HINARI - KAZAKHSTAN, Wiley Online Library on [01/04/2026]. See the Terms and Conditions (https://onlinelibrary.wiley.com/terms-and-conditions) on Wiley Online Library for rules of use; OA articles are governed by the applicable Creative Commons License

[34] W. J. Nimens, S. J. Lefave, L. Flannery et al., "Understanding hydrogen bonding interactions in crosslinked methylammonium lead iodide crystals: towards reducing moisture and light degradation pathways," *Angewandte Chemie International Edition*, vol. 58, no. 39, pp. 13912–13921, 2019.

[35] J. Mizusaki, K. Arai, and K. Fueki, "Ionic conduction of the perovskite-type halides," *Solid State Ionics*, vol. 11, no. 3, pp. 203–211, 1983.

[36] J. M. Azpiroz, E. Mosconi, J. Bisquert, and F. De Angelis, "Defect migration in methylammonium lead iodide and its role in perovskite solar cell operation," *Energy & Environmental Science*, vol. 8, no. 7, pp. 2118–2127, 2015.

[37] C. Eames, J. M. Frost, P. R. F. Barnes, B. C. O'Regan, A. Walsh, and M. Saiful Islam, "Ionic transport in hybrid lead iodide perovskite solar cells," *Nature Communications*, vol. 6, Article ID 7497, 2015.

[38] M. Bag, L. A. Renna, R. Y. Adhikari et al., "Kinetics of ion transport in perovskite active layers and its implications for active layer stability," *Journal of the American Chemical Society*, vol. 137, no. 40, pp. 13130–13137, 2015.

[39] B. Saparov and D. B. Mitzi, "Organic–inorganic perovskites: structural versatility for functional materials design," *Chemical Reviews*, vol. 116, no. 7, pp. 4558–4596, 2016.

[40] L. Yang, Y. Chen, X. Wang et al., "First-principles study on the stability and electronic properties of Dion–Jacobson halide A′ $(MA)_{n-1}B_nX_{3n+1}$ perovskites," *The Journal of Physical Chemistry C*, vol. 125, no. 43, pp. 24096–24104, 2021.

[41] Y. Chen, X.-L. Ding, H.-B. He et al., "Divalent organic cations as a novel protective layer for perovskite materials," *Journal of Materials Chemistry A*, vol. 11, no. 22, pp. 11684–11695, 2023.

[42] Y. Chen, X. Ding, L. Yang et al., "Small practical cluster models for perovskites based on the similarity criterion of central location environment and their applications," *Physical Chemistry Chemical Physics*, vol. 24, no. 23, pp. 14375–14389, 2022.

9182, 2023, 1, Downloaded from https://onlinelibrary.wiley.com/doi/10.1155/2023/6279023 by INASP/HINARI - KAZAKHSTAN, Wiley Online Library on [01/04/2026]. See the Terms and Conditions (https://onlinelibrary.wiley.com/terms-and-conditions) on Wiley Online Library for rules of use; OA articles are governed by the applicable Creative Commons License